

# Constraints on the spectra of $^{17,19}\text{C}$

S. Karataglidis<sup>(1),\*</sup> K. Amos<sup>(2),†</sup> P. Fraser<sup>(2),‡</sup> L. Canton<sup>(3),§</sup> and J. P. Svenne<sup>(4),¶</sup>

<sup>(1)</sup>*Department of Physics and Electronics, Rhodes University,  
P.O. Box 94, Grahamstown 6140, South Africa*

<sup>(2)</sup>*School of Physics, University of Melbourne, Victoria 3010, Australia*

<sup>(3)</sup>*Istituto Nazionale di Fisica Nucleare, sezione di Padova,  
e Dipartimento di Fisica dell'Università di Padova,  
via Marzolo 8, Padova I-35131, Italia and*

<sup>(4)</sup>*Department of Physics and Astronomy, University of Manitoba,  
and Winnipeg Institute for Theoretical Physics,  
Winnipeg, Manitoba, Canada, R3T 2N2*

(Dated: September 16, 2008)

## Abstract

Diverse means are used to investigate the spectra of the radioactive, exotic ions,  $^{17,19}\text{C}$ . First, estimates have been made using a shell model for the systems. Information from those shell model studies were then used in evaluating cross sections of the scattering of 70A MeV  $^{17,19}\text{C}$  ions from hydrogen. Complementing those studies, a multichannel algebraic scattering (MCAS) theory for  $n+^{16,18}\text{C}$  coupled-channel problems has been used to identify structures of the compound systems. The results show that the shell model structure assumed for these ions is reasonable with little need of effective charges. The conditions that two excited states exist within a few hundred keV of the ground state places some restriction upon the structure models. Other positive parity states are expected in the low-lying spectra of the two nuclei.

PACS numbers: 21.10.Hw, 25.30.Dh, 25.40.Ep, 25.80.Ek

---

\*Electronic address: S.Karataglidis@ru.ac.za

†Electronic address: amos@physics.unimelb.edu.au

‡Electronic address: pfraser@physics.unimelb.edu.au

§Electronic address: luciano.canton@pd.infn.it

¶Electronic address: svenne@physics.umanitoba.ca

## I. INTRODUCTION

The properties of nuclei at and near to the nucleon drip lines are the subject of some current interest as, increasingly, exotic nuclei are being produced in radioactive ion beams (RIB) with which scattering experiments can be made. Particular interest lies with such nuclei that have large neutron (or proton) excess distributed in the extended spatial manner termed a nucleon halo [1]. The neutron-rich carbon and oxygen isotopes are of special interest with the conjecture that variation of deformation of their ground states point to a new magic number of 16. Another conjecture is that the ground state deformation is neutron number dependent. That is suggested by deformed Hartree-Fock studies [2] from which the isotopes  $^{15,16,17}\text{C}$  are expected to have prolate deformation. However, with  $^{19}\text{C}$ , prolate and oblate deformations were found to be almost degenerate.

The neutron-rich nuclei  $^{17,19}\text{C}$  are two exotic nuclear systems that have received some attention recently. Of note is that they have been used in RIB, at 70A MeV energy, and cross sections measured [3] in scattering from hydrogen targets. While both nuclei have large neutron excess,  $^{19}\text{C}$  is of particular interest since it lies at the drip line, has a small single-neutron separation energy,  $\sim 0.53$  MeV, and most likely can be classified as a one-neutron halo nucleus [4]. However, the spin-parity of its ground state is still uncertain. A standard shell model (SM) [5] gave a  $\frac{1}{2}^+$  assignment making the nucleus a candidate to be a  $1s_{\frac{1}{2}}$ -neutron-halo nucleus. This is also suggested from studies of the Coulomb dissociation of  $^{19}\text{C}$  in collisions with heavy mass targets (Ta and Pb) [4, 6]. The same conjecture regarding the ground state, and suggestions of the spin-parities of low-lying excited states, were given in the recent study by Elekes *et al.* [7]. Their predictions were based upon SM evaluations, though in their paper they show only a few of the possible states. We have made independently an SM calculation to get a spectrum of  $^{19}\text{C}$  using the code OXBASH [8] with the WBP [9] interactions and within the *spstdpf* model space. From that calculation we found that there may be more than one candidate for the ground state.

An alternative approach has been used by Ridikas *et al.* [10, 11] to obtain the states in  $^{17,19}\text{C}$  as a neutron coupled to a core in a coupled-channels model. Their results suggested that  $^{19}\text{C}$  in its ground state qualified as a neutron-halo and would have either a  $\frac{1}{2}^+$  or a  $\frac{3}{2}^+$  spin-parity assignment. The  $\frac{5}{2}^+$  option was deemed unlikely. They also noted that coupled-channel effects were important in this description. But there is a possible problem with that since assurance of the Pauli principle is not guaranteed with their approach. Such assurance is feasible within the MCAS scheme [12] and how important that is has been demonstrated in Refs. [13, 14, 15]. We will show the extent of that problem with  $^{19}\text{C}$  herein. Notably in this case blocking of the  $0s_{\frac{1}{2}}$ ,  $0p_{\frac{3}{2}}$ ,  $0p_{\frac{1}{2}}$ , and (at least partially) the  $0d_{\frac{5}{2}}$  and  $1s_{\frac{1}{2}}$ -orbitals, which Ridikas *et al.* [10, 11] have not ensured, has impact.

Nucleon-nucleus scattering at medium energies, which under inverse kinematics equates to scattering of nuclei from hydrogen targets, is an excellent means by which the matter density of the nucleus may be studied. Microscopic models now exist with which predictions of data from both elastic and inelastic scattering reactions can be made. When good, and detailed, specification of the nucleonic structure of the nucleus is used, those predictions usually agree very well with observation [16], both in shape and magnitude. To facilitate such analyses of data, one first must specify the nucleon-nucleus ( $NA$ ) interaction. To do so requires two main ingredients: a) an effective nucleon-nucleon ( $NN$ ) interaction in-medium, allowing for the mean field as well as Pauli-blocking effects; and b) a credible model of structure of the nucleus that is nucleon-based. The process of forming optical potentials

in this way has been termed  $g$ -folding [16]. With relative motion wave functions defined using  $g$ -folding potentials, a distorted wave approximation (DWA) suffices to analyze most inelastic scattering data. With such conditions met, past studies of the scattering (elastic and inelastic) of helium and lithium isotopes from hydrogen targets [16, 17, 18] revealed that  ${}^6\text{He}$  and  ${}^{11}\text{Li}$  could be characterised as neutron halo nuclei while  ${}^8\text{He}$  and  ${}^9\text{Li}$  were not. However, the latter pair was seen to have their neutron excess as a skin-like distribution. The differential cross sections from both elastic and inelastic scattering of those ions from hydrogen had signatures of those excess neutron distributions.

In the next section, we specify details of the SM calculations for  ${}^{17,19}\text{C}$  we have made, and compare the spectra with the few states of these systems that are known. We also specify other properties of these systems, such as root mean square radii. In Sec. III we consider the nuclei as coupled-channel problems of a neutron on  ${}^{16,18}\text{C}$ , allowing coupling to the ground and  $2^+$  excited states in particular. The sensitivity to aspects of the coupling interaction are delineated and the crucial effect of Pauli blocking and hindrance with these coupled-channel studies is highlighted. Then in Sec. IV the results of DWA analyses of the scattering of 70A MeV  ${}^{17,19}\text{C}$  ions from hydrogen are compared with the recently available data [3]. Conclusions are then given in Sec. V.

## II. THE SHELL MODEL AND ${}^{17,19}\text{C}$

The spectra of  ${}^{17}\text{C}$  and  ${}^{19}\text{C}$ , as obtained from the SM calculations made using the WBP interaction [9], are displayed in Fig. 1. Only positive parity states are shown since there is no knowledge to date of any states of negative parity. The shell-model spectrum of  ${}^{17}\text{C}$  has a ground state whose spin-parity and isospin assignment ( $J^\pi; T$ ) is  $\frac{3}{2}^+; \frac{5}{2}$ . Then the first excited state at 32 keV has spin-parity  $\frac{5}{2}^+$ . Note that a small perturbation in the matrix elements in the interaction may invert these states. The same ordering of states is also observed in the spectrum obtained using the MK3W interaction, but the first excited state is at 218 keV. A low-energy spectrum for  ${}^{17}\text{C}$  was measured by Elekes *et al.* [7], wherein two excited states were observed: one at 210 keV and the other at 331 keV. Those were given tentative assignments of  $\frac{1}{2}^+$  and  $\frac{5}{2}^+$  respectively, compared to the ground state specification of  $\frac{3}{2}^+$ . Our result confirms that of Ref. [7] and which they designate as the *psdwbp* shell-model result. That was also obtained using the WBP interaction. Higher excited states have been observed at 2.20, 3.05, and 6.13 MeV [3]. The states at 2.20 and 3.05 MeV have been given assignments of  $\frac{7}{2}^+$  and  $\frac{9}{2}^+$ , respectively, and we find equivalent states at 2.61 and 3.11 MeV. There is no evidence currently for excited states at 0.295 ( $\frac{1}{2}^+$ ), 2.00 ( $\frac{5}{2}^+$ ), and 2.90 ( $\frac{3}{2}^+$ ) MeV.

The observed spectrum of  ${}^{19}\text{C}$  [7] has a ground state with  $J^\pi; T = \frac{1}{2}^+; \frac{7}{2}$ . Then there are two excited states at 72 and 197 keV excitation. Those were assigned spins of  $\frac{3}{2}$  and  $\frac{5}{2}$  based on the assignments to states in  ${}^{17}\text{C}$ . A reversal of the spin assignments in  ${}^{17}\text{C}$  would also lead to the reversal of those in  ${}^{19}\text{C}$ . A higher excited state has been observed at 1.46 MeV [3], for which the assignment is  $\frac{5}{2}^+$ . Note that this is acknowledged as the second  $\frac{5}{2}^+$  state [3], consistent with our shell-model predictions.

As a first test of the model of structure, one can evaluate various root mean square (rms) radii. With radioactive nuclear ions one can link their matter rms radii to the reaction cross sections from their scattering off stable target nuclei [19]. In general, though, there

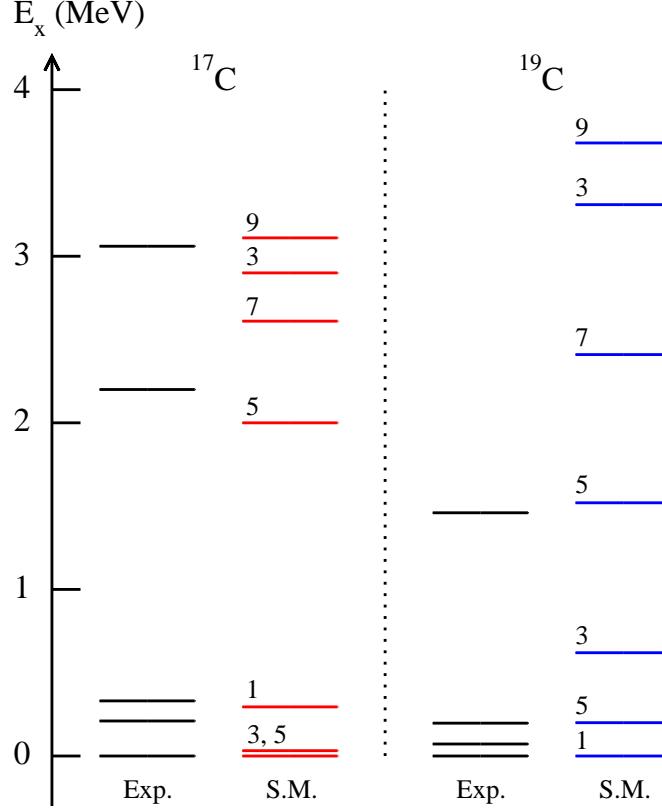


FIG. 1: (Color online.) The spectra of  $^{17,19}\text{C}$  generated from our SM calculations with the WBP potentials compared to experimental values. The number identifying each (positive parity) state is  $2J$  (twice the spin of the state).

are problems in doing so reliably as the usual methods of analysis, using Glauber theory of scattering and making additional approximations, can lead to disparate results. That is especially so if the ion in question has weakly bound neutrons that give it an extended neutron matter distribution. Such was found for  $^{19}\text{C}$  in particular [20]. In that study, both the optical limit (OL) and few-body (FB) approximations were used to analyze the reaction cross sections of  $^{19}\text{C}$  ions scattering from  $^{12}\text{C}$ . As shown in their Fig. 5, with a neutron separation energy of 0.5 MeV, the reaction cross section data gave rms radii of  $\sim 2.97$  and  $\sim 3.12$  fm when analyzed using the OL and FB schemes respectively. Using Glauber theory to analyze their interaction cross section data, Ozawa *et al.* [19] found values of  $\sim 2.72$  fm for the matter rms radius of  $^{17}\text{C}$  and of 3.13 fm (OL) and 3.23 fm (FB). However, from an analysis of the reaction cross sections from the scattering of  $^{17,19}\text{C}$  ions from  $^{\text{nat}}\text{Cu}$  made using Karol's prescription [21], Liatard *et al.* [22] deduced matter rms radii of 3.04 and 2.74 fm for the  $^{17,19}\text{C}$  ions respectively. The latter results imply that  $^{17}\text{C}$  would have a more extended neutron distribution than  $^{19}\text{C}$ .

In Table I the experimental rms matter radii for  $^{17}\text{C}$  and  $^{19}\text{C}$  ions assessed from their interaction cross sections from  $^{12}\text{C}$  targets, the FB and OL method results, are compared with the pure SM results we have found and with a model prescription defined in ref. [23]. The SM results are given in the columns identified by 'WBP' and were obtained using the WBP interaction and harmonic oscillator single particle wave functions ( $b = 1.6$  fm) to

TABLE I: Root mean square radii (in fm) for  $^{17,19}\text{C}$ .

Nucleus	$\sqrt{\langle r_C^2 \rangle}$	$\sqrt{\langle r_T^2 \rangle}$		
	WBP	WBP	Ref. [23]	Expt. [19]
$^{17}\text{C}$	2.425	2.500	3.1	$2.72 \pm 0.04$
$^{19}\text{C}$	2.422	2.556	3.7	$3.23 \pm 0.08$ (FB)
				$3.13 \pm 0.07$ (OL)
$^{19}\text{C}$ (halo)	2.699	3.982		

specify the shell-model Hamiltonians. The evaluated charge ( $\sqrt{\langle r_C^2 \rangle}$ ) and matter ( $\sqrt{\langle r_T^2 \rangle}$ ) radii are given. Clearly the evaluated radii are too small whatever the experimental values should be. But one must remember that heavy-ion collisions are mostly peripheral and methods of extraction of the radii from such are subject to some uncertainty aside from the quoted errors that relate to data. Nonetheless it has been anticipated from studies of neutron break-up reactions [24] that  $^{19}\text{C}$  is a one-neutron halo system. In these studies we can have a density profile that is neutron-halo-like by using Woods-Saxon (WS) single-nucleon bound-state wave functions. The WS potential chosen was that used in the past for  $^{12}\text{C}$ , but with the most important *sd* (valence) orbits having weak binding energy (0.53 MeV [4]). Similar considerations [17, 18] lead to a neutron halo description for  $^6\text{He}$ . Doing so with the SM ground state one-body-density-matrix-elements (OBDME) [16], gave an rms matter radius for  $^{19}\text{C}$  of 3.982 fm as listed in the row of Table I defined by  $^{12}\text{C}$  (halo). The associated charge radius is slightly larger also. A cluster model calculation [23], based on the separation energy of the valence neutron, gave 3.1 and 3.7 fm for the matter radii of  $^{17}\text{C}$  and  $^{19}\text{C}$ , respectively. Those are listed in Table I under the column heading of Ref. [23]. Our halo result for the matter radius of  $^{19}\text{C}$  is consistent with that result, but both are much higher than the experimental values.

Recently [25], reaction cross sections of  $^{17,19}\text{C}$  as RIB scattering from hydrogen were shown to be a good measure of spatial distributions of neutron excess in many exotic nuclei. That was so because that scattering probes more of the nuclear interior than does heavy ion collisions and the method of analysis was based upon a credible, microscopic reaction theory using realistic models of the structure of the ions. We have used the same approach, folding the relevant Melbourne effective, medium modified, *NN* interactions [16] with the structure details given by the shell model, to predict elastic scattering cross sections for 70A MeV  $^{17,19}\text{C}$  ions from hydrogen. With oscillator single nucleon bound state wave functions, those calculations gave 423 and 461 mb for the relevant reaction cross sections. Using the WS (halo creating) set of bound state functions, the reaction cross section of the  $^{19}\text{C}$  scattering was 584 mb. The much higher value of the reaction cross section from the WS (halo) model is consistent with that found for  $^6\text{He}$ , where such was needed to reproduce the measured value [17]. A measurement of the reaction cross section for the scattering of  $^{19}\text{C}$  from hydrogen would therefore be desirable.

The differential cross sections, themselves, are shown and discussed later in Sec. IV.

### III. $^{17,19}\text{C}$ AS A COUPLED-CHANNEL PROBLEM OF $n+^{16,18}\text{C}$

Herein we report evaluations of spectra for  $^{17,19}\text{C}$  that have been defined from coupled-channel calculations of the nucleon-core,  $n+^{16,18}\text{C}$  systems, using the multi-channel algebraic scattering (MCAS) method [12, 26, 27]. The method is given in detail in those references and so is not presented again. Of great importance in the MCAS approach is that Pauli blocking or hindrance can be accommodated in the Hamiltonian [14], even if a collective model is used to define the coupling interactions. In the collective model, such can be achieved by using an orthogonalizing pseudo-potential (OPP) scheme [26]; an approach used in defining spectra (bound states and resonances) for the mass-7 isobars [13] and of a nucleus just beyond the neutron drip-line,  $^{15}\text{F}$  [14]. However, while it is reasonable, with the  $^{16,18}\text{C}$  nuclei, to take the  $0s_{\frac{1}{2}}$ ,  $0p_{\frac{3}{2}}$ , and  $0p_{\frac{1}{2}}$ -neutron orbits to be totally blocked, we find that only partial blocking of the  $0d_{\frac{5}{2}}$ -neutron orbit is appropriate. Partial blocking, of the  $0p_{\frac{1}{2}}$ -orbit, was needed in an earlier study of the spectrum of mass-15 nuclei [14]. In these studies, the OPP strengths used were  $10^5$  MeV for the totally blocked states (essentially  $\infty$ ) but the neutron  $0d_{\frac{5}{2}}$ -orbit was hindered by using just a few MeV for the OPP strength in that orbit.

The MCAS program, to date, uses a collective model prescription for the input interaction potential matrix,  $V_{cc'}(r)$ ;  $c, c'$  representing the sets of quantum numbers that define each unique interaction channel [26]. Deformation of that interaction is taken to second order in the expansion scheme. Details of the interaction forms have been published [26]. The approach is as yet phenomenological with the attendant uncertainties in selection of parameter values though a microscopic approach based upon shell model wave functions and two-nucleon potentials is being developed. With stable target systems, usually there are many compound nucleus levels, bound and resonant, against which the coupling interaction can be tuned [26]. That is not the case with most exotic nuclei, at least currently. Indeed with  $^{17,19}\text{C}$  there are few known states in their spectra and the spin-parity assignments of those few are still uncertain. However, it does seem appropriate that both nuclei should have three states, including the ground state, within an excitation energy of a few hundred keV. One can reasonably expect those states to have spin-parity assignments of  $\frac{1}{2}^+$ ,  $\frac{3}{2}^+$ , and  $\frac{5}{2}^+$ , though in what order they occur is unclear with  $^{17}\text{C}$ . With  $^{19}\text{C}$  we will demand that the ground state has the  $\frac{1}{2}^+$  assignment, in line with recent arguments [3] that this nucleus has a very extended neutron distribution designated as a neutron halo. Likewise, while there is a reasonably known low-excitation spectrum for  $^{16}\text{C}$ , not much is known of the spectrum of the target nucleus  $^{18}\text{C}$ .

Consequently the channels chosen for the coupling in the  $n+^{16,18}\text{C}$  studies have been limited to the ground,  $0^+$ , and a  $2^+$ . Excitation energies of that  $2^+$  state were taken from the compilations [28, 29] as 1.77 and 1.62 MeV for  $^{16,18}\text{C}$  respectively. There are three other states known in  $^{16}\text{C}$  lying below the  $n+^{15}\text{C}$  threshold with spin-parities thought to be  $0^+$ ,  $2^+$ , and  $4^+$  forming a triplet with average centroid energy  $\sim 3.4$  MeV. This is reminiscent of a vibrator spectrum with quadrupole phonon energy of  $\sim 1.7$  MeV and we view the two nuclei as such. Thus the triplet of states in  $^{16}\text{C}$ , and those we assume may be found eventually in  $^{18}\text{C}$ , we consider as two quadrupole phonon triplets which will couple weakly to the ground (vacuum) state. Hence we have ignored them in finding solutions of the coupled equations. By so restricting the problems to be one of two channels, we also relate to the model used by Ridikas *et al* [11]. The MCAS calculations leading to the spectra depicted in Figs. 2 and 4 were made using the parameter set listed in Table II. The geometries of the potentials were taken with  $R = 2.9$  fm and  $a = 0.8$  fm. These are not considered as either a unique

TABLE II: Parameter values used in MCAS evaluations of the spectra of  $^{17,19}\text{C}$ .

Nucleus	$V_0$ (MeV)	$V_{ls}$ (MeV)	$V_{ll}$ (MeV)	$V_{Is}$ (MeV)	$\beta_2$
$^{17}\text{C}$	-40.0	10.0	-2.5	2.0	0.3
$^{19}\text{C}$	-44.5	6.0	0.0	2.7	0.4

or even the best Hamiltonian potentials given the paucity of data against which we have to check. But they suffice to meet the limited constraints posed and to indicate on what the results are most sensitive. While only positive parity states are known (or suggested) in the spectra, taking the same interaction to define negative parity states, resonances of that parity are then found with MCAS evaluations to lie in this region of low-energy excitation. However, as there is no experimental information about any negative parity states in  $^{17,19}\text{C}$ , hereafter, in all figures and discussions, we only display and describe the positive parity spectra resulting from our calculations.

### A. The spectra of $^{17}\text{C}$

In Fig. 2, the currently known states in the spectrum of  $^{17}\text{C}$  are compared with the low excitation spectra for this nucleus that have been determined from a shell-model calculation (SM) and from the coupled-channel solutions (MCAS). The two theoretical calculations have very similar sets of states of spin-parity and both lead to two states within  $\sim 1$  MeV of the ground. The MCAS results are wider spread in energy than those found with the shell model. That spread persists despite the results being quite sensitive, in absolute binding as well as state order, to the deformation, the amount of  $0d_{5/2}$ -orbit blocking, and to the precise value of the spin-spin coupling,  $V_{Is}$ , in the interaction form. To illustrate, we show in Fig. 3, the variations of the spectra against each of those variables. We have not attempted to adjust other parameters seeking to regain the absolute binding energy of  $\sim 0.7$  MeV. In each panel, the individual states are associated with symbols as follows: the  $\frac{1}{2}^+$  state is shown by the filled circles, the  $\frac{3}{2}^+ \Big|_1$  state is shown by the filled squares, the  $\frac{5}{2}^+ \Big|_1$  state is shown by the open squares, the  $\frac{3}{2}^+ \Big|_2$  state is shown by the filled diamonds, the  $\frac{9}{2}^+$  state is shown by the open circles, the  $\frac{7}{2}^+$  state is shown by the open down triangles, and the  $\frac{5}{2}^+ \Big|_2$  state is shown by the open up triangles.

First consider the variations against the choice of the OPP strength for Pauli hindrance of the  $0d_{5/2}$  neutron orbit that are displayed in the top section of this figure. By and large the states simply track in parallel with increasing binding as the blocking is decreased. However the  $\frac{3}{2}^+$  states show a coupling effect, similar to orbit repulsion, in the 3 to 4 MeV strength range, to alter the positions of those two states in the spectrum relative to others.

In the middle panel of Fig 3, the variation of the evaluated spectrum of  $^{17}\text{C}$  is shown as the deformation parameter,  $\beta_2$ , is changed. This variation of MCAS results has been used previously [15] to ascertain not only how the channel coupling mixes basis states to optimally give a compound nucleus spectrum, but also to delineate the basis state that is the progenitor of each compound system one. In the case of  $^{17}\text{C}$  the two most bound states, having spin-parity of  $\frac{5}{2}^+$  and  $\frac{1}{2}^+$ , remain close to each other whatever the deformation value.

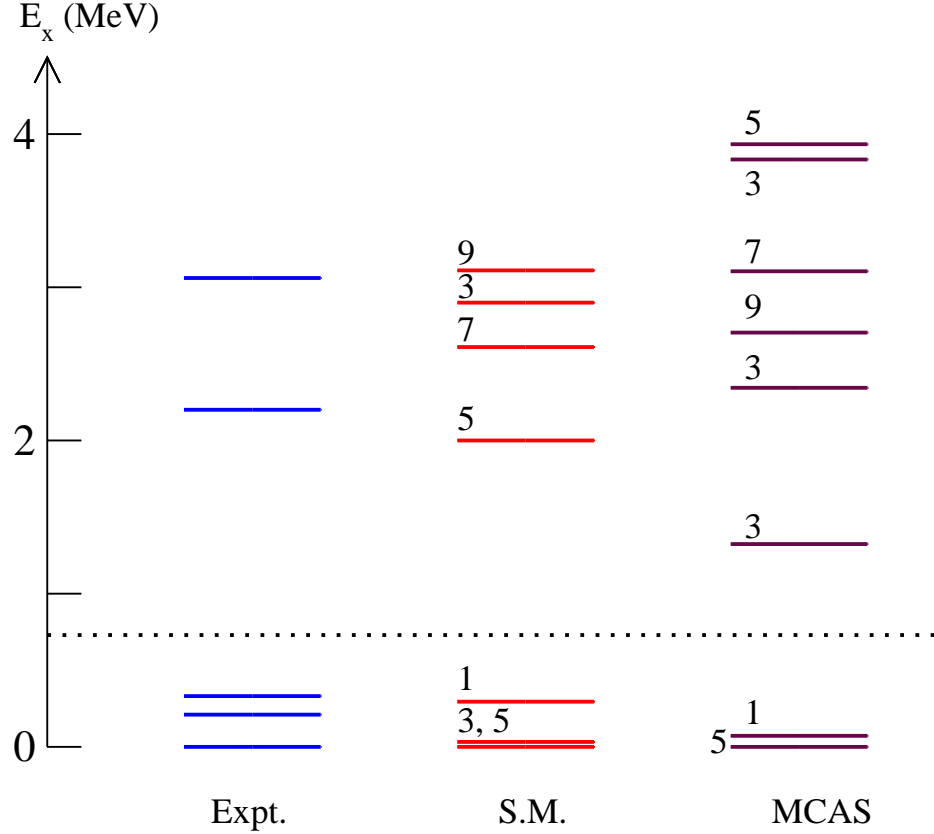


FIG. 2: (Color online.) The low excitation spectrum of  $^{17}\text{C}$ . The data are compared with the results of a  $2\hbar\omega$  SM calculation and with a spectrum determined using the MCAS approach. The dotted line indicates the  $n+^{16}\text{C}$  threshold. The numeral identifying each state is again  $2J$ .

With increasing deformation, the other states in the spectrum spread apart.

Finally, in the bottom panel we display the variation of the spectrum with changes of the spin-spin,  $V_{Is}$ , term in the Hamiltonian. Most states in the spectrum track more or less parallel in energy with increasing interaction spin-spin strength. The exceptions are the  $\frac{9}{2}^+$  resonance state which increases its centroid energy and the ground state whose energy hardly changes at all.

### B. The spectra of $^{19}\text{C}$

In Fig. 4 the currently known states [3, 7] in the spectrum of  $^{19}\text{C}$  are compared with the low excitation spectra for this nucleus determined from a SM calculation and with that found from the coupled-channel solutions (MCAS) based upon a two-state, collective, model for the  $n+^{18}\text{C}$  system. In this case, the OPP strength of the neutron  $0d_{\frac{5}{2}}$ -orbit was chosen as 100 MeV. Since that orbit is expected to have more neutrons contained than in  $^{17}\text{C}$ , variation of the  $d_{\frac{5}{2}}$  blocking did not give as dramatic a change in the spectra, until the strength of the OPP for that orbit was reduced to a value of 10 MeV or less. Then only the ground state ( $\frac{1}{2}^+$ ) binding energy was noticeably affected by being more bound by a few hundreds of keV. However, taking the  $d_{\frac{5}{2}}$  orbit to be Pauli allowed, introduced spuriousity



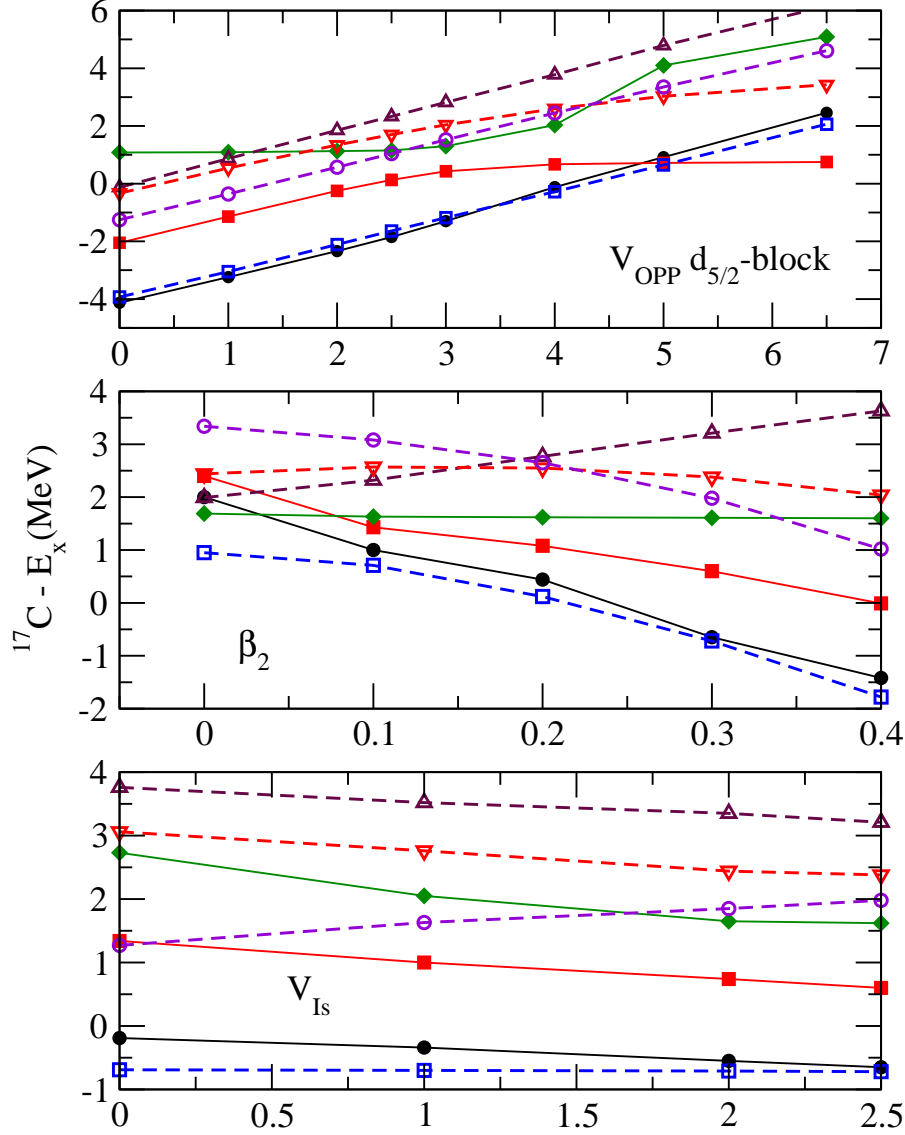


FIG. 3: (Color online.) The low excitation spectrum of  $^{17}\text{C}$  from MCAS results found by varying the OPP for  $0d_{5/2}$ -orbit blocking (units are MeV), the deformation strength,  $\beta_2$ , and the spin-spin coupling,  $V_{\text{Is}}$  (units are MeV) in the Hamiltonian. The various lines are as described in the text.

and the  $\frac{1}{2}^+$  no longer is the ground state. This is discussed more in the next section.

The variation of the spectrum found by varying the deformation parameter  $\beta_2$  is displayed in Fig. 5. An equally dramatic, but quite different, variation of results with  $\beta_2$  was also found in a study [15] of the spectrum of  $^{13}\text{C}$  treated as a coupled-channel,  $n+^{12}\text{C}$ , system. The excitation energies of the states all vary regularly as the deformation increases, either for prolate (positive  $\beta_2$ ) or oblate (negative  $\beta_2$ ) character. Two states stand out as being dominantly the coupling of a single neutron to the ground state of  $^{18}\text{C}$ . They are denoted by the filled circles (lowest set) being the ground state of  $^{19}\text{C}$  formed (when  $\beta_2 = 0$ ) with a  $1s_{1/2}$ -neutron, and by the filled triangles being a state formed (when  $\beta_2 = 0$ ) with a  $\frac{5}{2}^+$ -neutron. These states vary with deformation noticeably more slowly than the others. That is so especially for the ground state reflecting that the prime admixing component (the

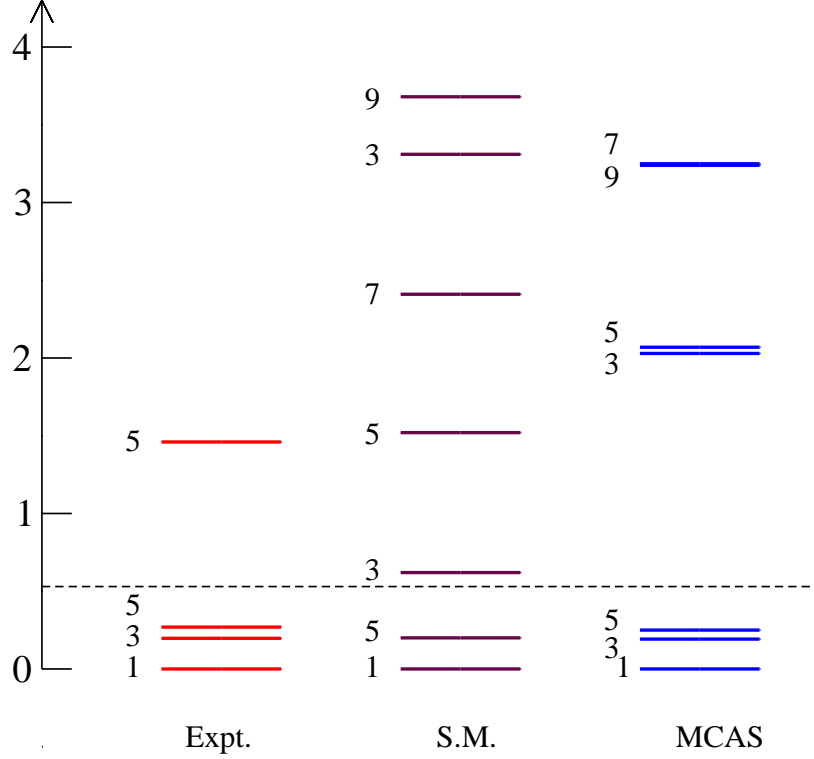


FIG. 4: (Color online.) The low excitation spectrum of  $^{19}\text{C}$ . The data [3, 7] are compared with the results of a  $2\hbar\omega$  SM calculation (SM) and with a spectrum found using the MCAS approach. The dashed line indicates the  $n+^{18}\text{C}$  threshold, while the numeral identifying each state is again  $2J$ .

$\left[0d_{\frac{5}{2}} \otimes 2^+\right]_{\frac{1}{2}})$  lies above 4 MeV in the unperturbed spectrum. But it is important to note that the deformation coupling mixes all basic states of given spin-parity to form the resultant ones in the spectrum of  $^{19}\text{C}$ . Thus Ridikas *et al.* [11] ascertained that the ground state could have as much as 25% mixing of  $0d \otimes 2^+$  with the basic  $1s \otimes 0_{\text{g.s.}}^+$  component. From this plot it is also clear that our coupled-channel calculations require a strong deformation  $\sim 0.4$  to obtain three states of the appropriate spin-parity lying below the neutron- $^{18}\text{C}$  threshold and still retaining a one-neutron separation energy of  $\sim 0.53$  MeV.

The resonance states, found using MCAS and the deformation  $\beta_2 = 0.4$ , have neutron widths of 0.35 MeV  $\left(\frac{3}{2}^+ \Big|_2\right)$ , 2.6 MeV  $\left(\frac{5}{2}^+ \Big|_2\right)$ , 0.47 MeV  $\left(\frac{9}{2}^+\right)$ , and of 0.71 MeV  $\left(\frac{7}{2}^+\right)$ . If these widths are credible, then it is more likely that the cross section measured by Satou *et al.* [3] in the scattering of 70A MeV  $^{19}\text{C}$  ions from hydrogen is the excitation of the  $\frac{5}{2}^+ \Big|_2$  state. Structure models then have to find that state  $\sim 1$  MeV lower in energy.

The strength of the spin-spin interaction,  $V_{I.s}$ , is non-zero so that, when  $\beta_2 = 0$ , there is a splitting of the degeneracy of states basically formed by a particle coupling to the  $2_1^+$  state in  $^{18}\text{C}$ . Setting both  $\beta_2$  and the strength of the spin-spin ( $V_{I.s}$ ) to zero, gave the seven listed states but there are just four distinct state energies in the range. This limit gives the degeneracies that indicate the primary coupling of each listed state. Of course, with deformation, the eigenvalues of the Hamiltonian are admixtures of the primary states of

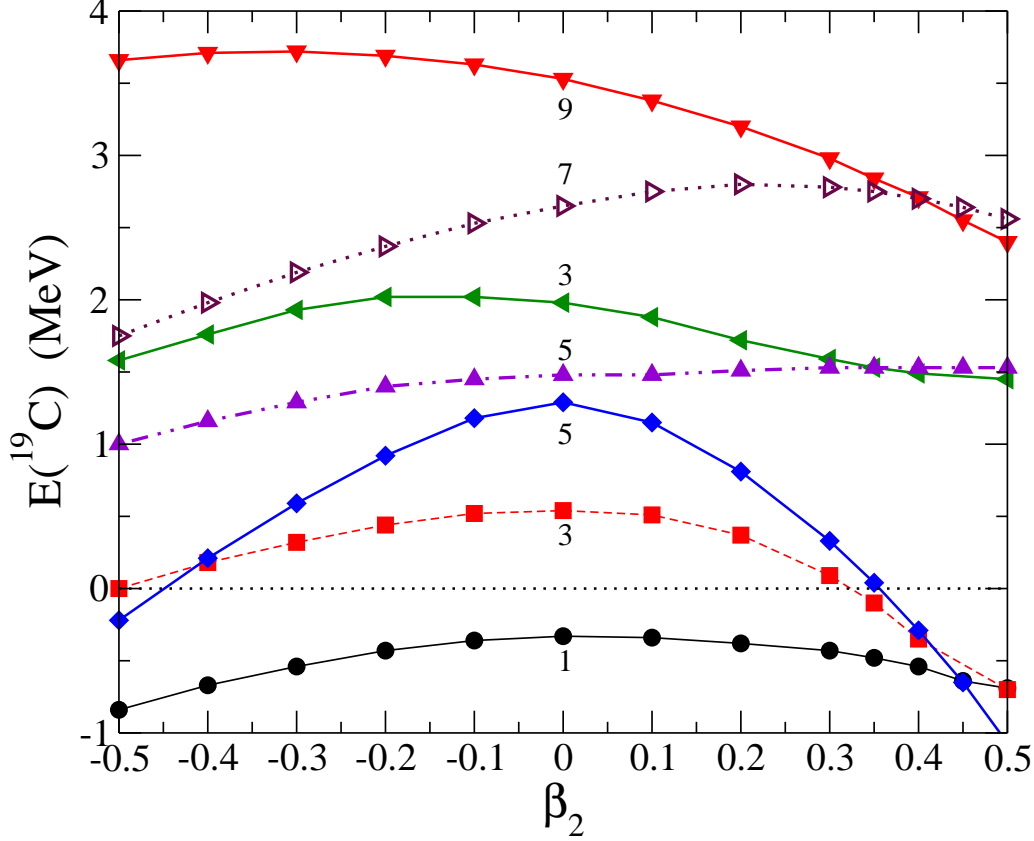


FIG. 5: (Color online.) The low excitation spectrum of  $^{19}\text{C}$  calculated with variation of the deformation  $\beta_2$ . The results for each spin-parity (in the order denoted in Fig. 4) are connected by lines drawn to guide the eye.

given  $J^\pi$ . The four resultant energies identify states ( $nl_j \otimes ^{18}\text{C}$ ) that are, with increasing energy,  $1s_{\frac{1}{2}} \otimes 0_{\text{g.s.}}^+$ , the doublet  $1s_{\frac{1}{2}} \otimes 2_1^+$ , a  $0d_{\frac{5}{2}} \otimes 0_{\text{g.s.}}^+$ , and a set that may originate from  $0d_{\frac{5}{2}} \otimes 2_1^+$ .

### C. Pauli blocking

We have shown in the foregoing discussion how changes occur in MCAS results when, using the OPP method, Pauli hindrance of the  $0d_{\frac{5}{2}}$ -orbit was made. In all of those analyses, the lower-lying single-particle orbits were taken to be Pauli blocked. With a collective model of interactions, the coupled-channel approach to define the spectrum of an  $(n + A)$  compound nucleus, we have shown previously [12, 13, 14, 15] how crucial it is to ensure that the Pauli principle is not violated in the analysis. We demonstrate how significant doing so is in one of the present cases. By not using the OPP in an MCAS evaluation of  $n+^{18}\text{C}$ , we find a plethora of states in the spectrum. The spectrum that results on using the best interaction potential (found for the problem with the OPP included) and then setting all of the OPP strengths to zero, is listed in Table III. In this solution of the coupled-channel problem, without taking the Pauli principle into account, the two most bound  $\frac{1}{2}^+$  states and the most bound  $\frac{3}{2}^+$  and  $\frac{5}{2}^+$  states are spurious. Even those other levels which might

TABLE III: Positive parity states in  $^{19}\text{C}$  formed when the Pauli principle is not enforced.

$J^{(+)}$	$\beta_2 = 0.4$	$\beta_2 = 0$	$\beta_2 = V_{ss} = 0$	Origin
$\frac{3}{2}^+$	-22.9	-22.9	-19.9	$0s_{\frac{1}{2}} + 2_1^+$
$\frac{1}{2}^+$	-21.7	-21.5	-21.5	$0s_{\frac{1}{2}} + 0_1^+$
$\frac{5}{2}^+$	-18.1	-18.2	-19.9	$0s_{\frac{1}{2}} + 2_1^+$
$\frac{1}{2}^+$	-2.02	-0.33	-0.33	$1s_{\frac{1}{2}} + 0_1^+$
$\frac{5}{2}^+$	-0.87	1.29	1.29	$0d_{\frac{5}{2}} + 0_1^+$
$\frac{3}{2}^+$	1.45	1.97	2.82	$0d_{\frac{5}{2}} + 2_1^+$
$\frac{5}{2}^+$	1.63	1.46	2.82	$0d_{\frac{5}{2}} + 2_1^+$
$\frac{1}{2}^+$	0.77	1.83	2.82	$0d_{\frac{5}{2}} + 2_1^+$
$\frac{9}{2}^+$	2.39	3.53	2.82	$0d_{\frac{5}{2}} + 2_1^+$
$\frac{7}{2}^+$	2.56	2.65	2.82	$0d_{\frac{5}{2}} + 2_1^+$

be associated with actual states of the system, would have spurious components in their wave functions [12, 15, 30]. A similar large set of spurious negative parity states were found when the negative parity interaction was taken to be the same as that for the positive parity study.

#### IV. ELASTIC AND INELASTIC SCATTERING OF 70A MEV IONS

We have used a  $g$ -folding model to specify the optical potentials with which predictions of elastic scattering observables have been made. Those potentials then have been used to find the distorted waves that we use in DWA calculations of inelastic scattering. The effective two-nucleon interaction used in the  $g$ -folding was also used as the transition operator effecting the inelastic transitions. Full details are given in Ref. [16] and so are not repeated herein.

##### A. The elastic scattering

Our  $g$ -folding model results for the elastic scattering cross sections (the kinematic inverse equivalent of 70A MeV  $^{17,19}\text{C}$  ions from hydrogen) are shown in Fig. 6. As indicated, the top set of results are for  $^{17}\text{C}$  scattering, the middle set are for  $^{19}\text{C}$ , and in the bottom panel we compare the results for the two nuclei. In the top panel, there are three results shown for  $^{17}\text{C}$ . Of those, the solid curve is the total result found assuming that the ground state has spin-parity of  $\frac{3}{2}^+$ . A number of multipoles ( $L = 0, 1, 2, 3$ ) contribute to the scattering, and while the monopole term is defined from the  $g$ -folding optical potential, the other multipole contributions have been found using a DWA method [16]. In all though, the input information (OBDME and single nucleon wave functions, oscillators with  $b = 1.6$  fm) was obtained from our SM calculations made using the WBP potentials. The dashed curve is the result when only the  $L = 0$  components in that full calculation are retained. When the (monopole) OBDME determined by using the MK3W potentials in a shell-model calculation are used, the cross section can hardly be distinguished from this dashed curve. The dot-

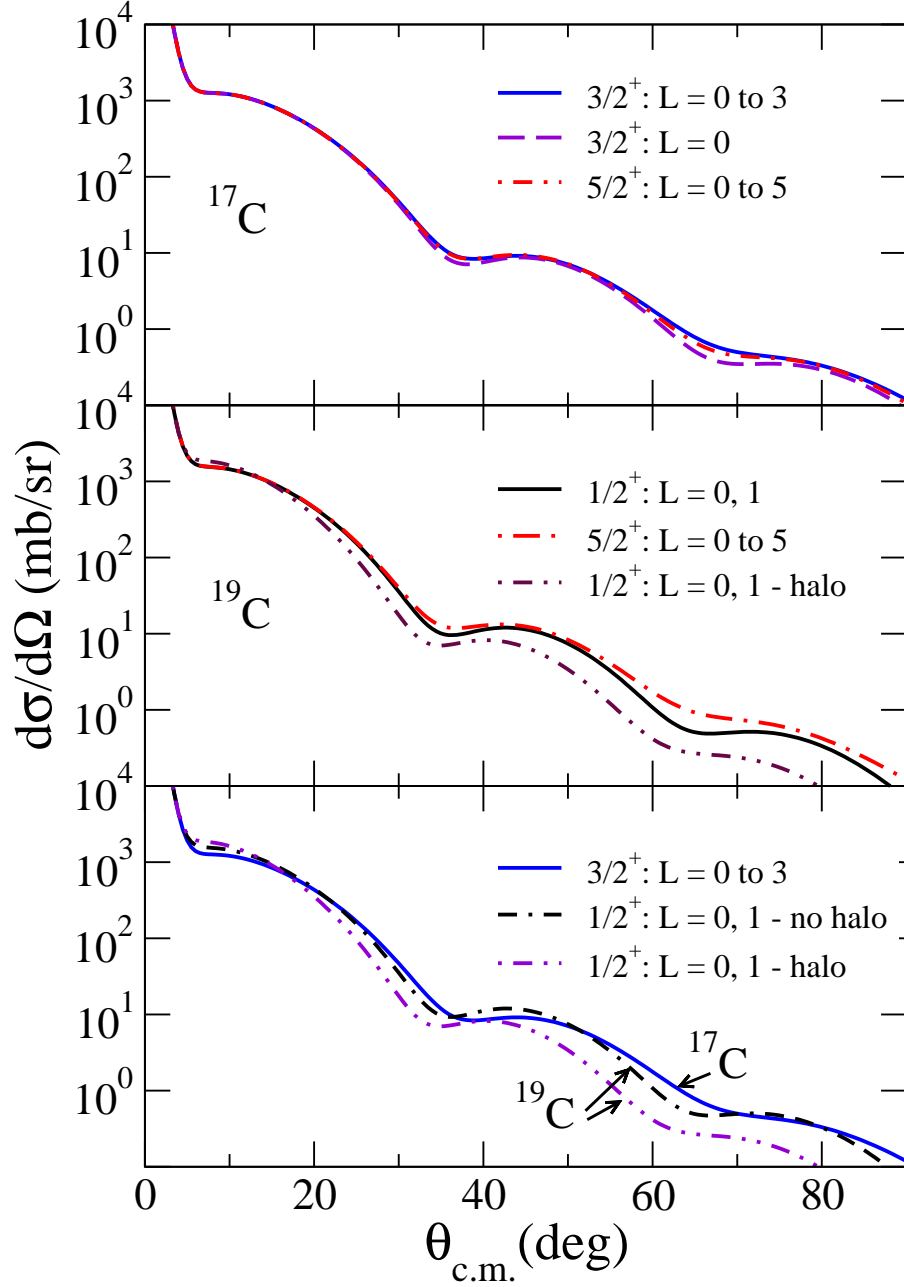


FIG. 6: (Color online.) The differential cross sections for the elastic scattering of 70A MeV  $^{17,19}\text{C}$  ions from hydrogen. The legends identify what spin-parity has been assumed for the ground states, and what transition multipoles have been taken into account. More details are given in the text.

dashed curve is the total result found using OBDME from a SM calculation made with the WBP potentials but assuming that the ground state has the  $\frac{5}{2}^+$  specification. There is very little difference among all of these results indicating that the monopole terms dominate; that the choice of SM potentials is not discernible (in the elastic scattering cross section); and that the results do not show a preference for either the  $\frac{3}{2}^+$  or  $\frac{5}{2}^+$  choice of spin-parity of the ground state.

In the middle panel are the results for the elastic scattering of 70A MeV  $^{19}\text{C}$  ions from

hydrogen which were also found using the WBP SM information. The solid curve depicts the result found assuming that the ground state has a spin-parity assignment of  $\frac{1}{2}^+$ . Almost the same result was found when the ground state was taken to have a spin-parity assignment of  $\frac{5}{2}^+$  though only if a monopole interaction contribution is considered. Allowing for all multipole contributions with a  $\frac{5}{2}^+$  assignment, with amplitudes for non-zero multipoles obtained using the DWA, lead to the result shown by the dot-dashed curve. There is some difference according to what is assumed for the ground-state spin-parity in this case, more than seen with  $^{17}\text{C}$ , but the differences overall remain small and it may be too hard to discern experimentally. Again, the single-nucleon wave functions used were harmonic oscillators with  $b = 1.6$  fm. To consider whether  $^{19}\text{C}$  is a halo, we have also made evaluations with the single-nucleon wave functions being those of the WS potential specified earlier. The neutron density formed with such wave functions is quite extended; to form what has been termed a neutron halo. Of course, even with oscillator wave functions, these nuclei ( $^{17,19}\text{C}$ ) have neutron skins. However, on using the WS functions in the  $g$ -folding process, optical potentials result from which the cross section depicted by the dot-dot-dashed curve in the middle panel of Fig. 6. It differs sufficiently from the cross section found using the oscillator wave functions that measurement should reflect which, if either, is the more appropriate. Regrettably, no data for this elastic scattering have been taken.

Finally, in the bottom panel, we compare the cross sections we have evaluated for the two nuclei. Assuming that the spin-parities of the ground states are  $\frac{3}{2}^+$  and  $\frac{1}{2}^+$  for  $^{17,19}\text{C}$  respectively, the solid curve is the  $^{17}\text{C}$  scattering cross section. The other two are the  $^{19}\text{C}$  cross sections found using oscillator wave functions (dot-dash-dash curve) and the WS ones that form a neutron halo (dot-dot-dashed curve). The differences, especially if  $^{19}\text{C}$  has a neutron halo and  $^{17}\text{C}$  does not, should be observable.

## B. The inelastic scattering

Satou *et al.* [3] report data from the inelastic scattering of  $^{17,19}\text{C}$  ions from a hydrogen target. Differential cross sections from the scattering of 70A MeV ions leading to states at excitation energies of 2.2 and 3.05 MeV in  $^{17}\text{C}$  and to the 1.46 MeV excited state in  $^{19}\text{C}$  were presented. The analyses made in Ref. [3] suggest that the ground states have spin-parities of  $\frac{3}{2}^+$  ( $^{17}\text{C}$ ) and  $\frac{1}{2}^+$  ( $^{19}\text{C}$ ). Those authors also suggest that the excited states of  $^{17}\text{C}$  have spin-parity assignments of  $\frac{7}{2}^+$  (2.2 MeV) and  $\frac{9}{2}^+$  (3.05 MeV) while the 1.46 MeV state in  $^{19}\text{C}$  has a  $\frac{5}{2}^+$  specification. But it is unfortunate that no elastic scattering data have been taken, as replication of such by predictions is a first level of confidence as to the structure and single-nucleon wave functions that best describe the radioactive ion.

Past studies [17, 18] of scattering of the halo nucleus,  $^6\text{He}$ , from hydrogen showed that the extended neutron distribution for this ion, had a marked effect upon the elastic as well as the inelastic scattering cross sections. We proceed under the assumption that the results shown in Fig. 6 may replicate future data.

First we consider the inelastic scattering of 70A MeV  $^{17}\text{C}$  ions from hydrogen leading to a state in the radioactive ion at 2.2 MeV excitation. Data [3] for this excitation are displayed in Fig. 7. Assuming that the spin-parity of the excited state is  $\frac{7}{2}^+$  the DWA results in best agreement with this data were based upon the ground state having a spin-parity assignment of  $\frac{3}{2}^+$ . The complete result is depicted by the solid curve. The dashed curve is the result of using only the  $L = 2$  transfer contributions in the transition. Clearly

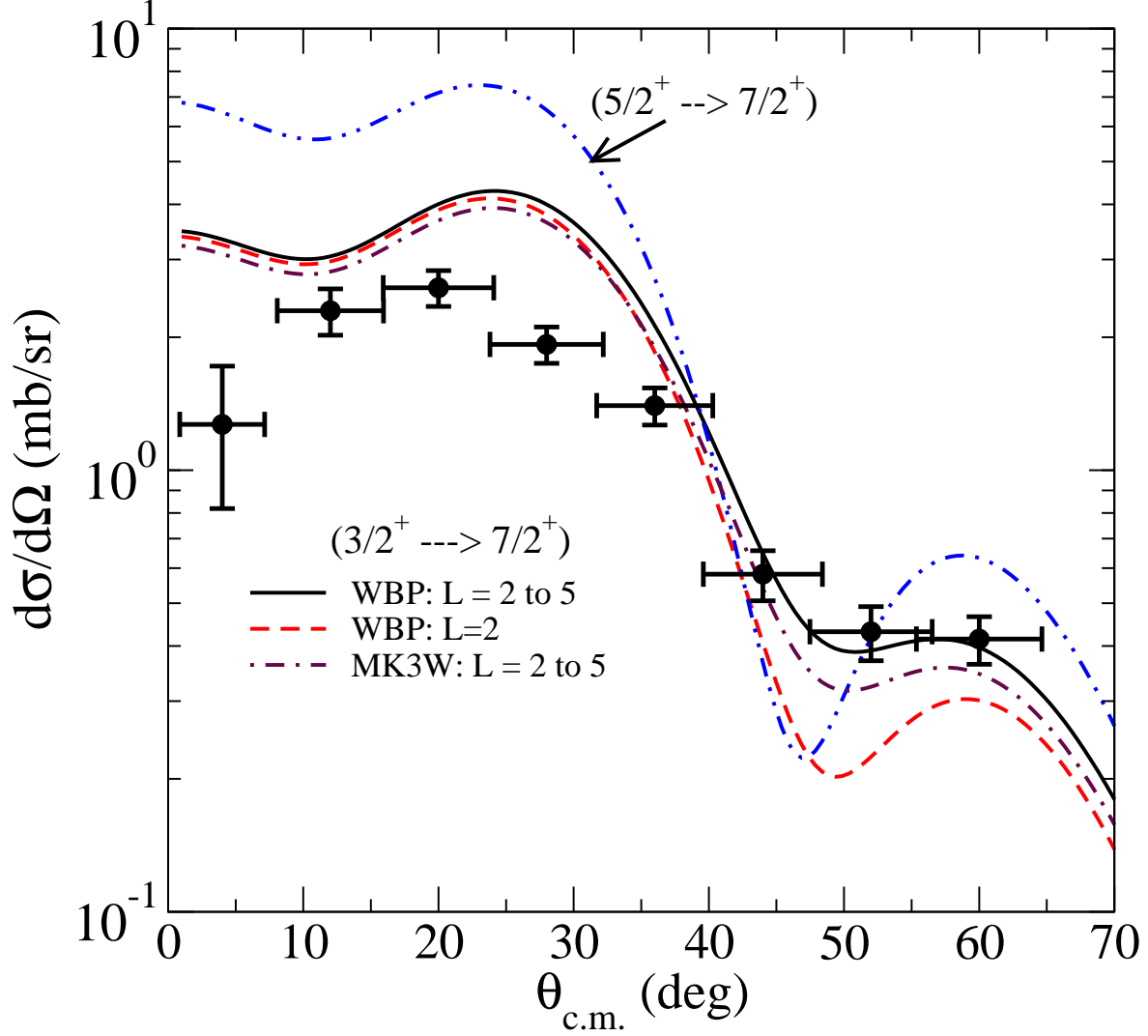


FIG. 7: (Color online.) The differential cross sections for the inelastic scattering of 70 MeV protons from  $^{17}\text{C}$  leading to the state at 2.2 MeV excitation. What has been assumed to be the spin-parities of the initial and final states in the transition are indicated in the brackets, while for the assumed  $\frac{3}{2}^+ \rightarrow \frac{7}{2}^+$  case, the legends indicate what shell model was used and what multipoles considered in the transition. More details are given in the text.

the  $L = 2$  transition dominates, and is in quite reasonable agreement with the observation. The third curve of this set, shown as the dot-dashed curve, is the cross section that results using the pure  $L = 2$  transition OBDME obtained from the shell-model calculation made using the MK3W interaction. The complete result found using that (MK3W) shell-model OBDME, is so similar to the solid curve that it is not shown. The fourth curve in Fig. 7, the dot-dot-dashed curve, portrays the cross section found when the ground state is assumed to have  $\frac{5}{2}^+$  spin-parity assignment. Comparisons with data clearly suggest the  $\frac{3}{2}^+$  spin-parity assignment for the ground state.

The state at 3.05 MeV excitation in  $^{17}\text{C}$  is assumed to have a spin-parity of  $\frac{9}{2}^+$ , and cross-section data from its excitation in the collision of 70A MeV  $^{17}\text{C}$  ions with hydrogen [3] are displayed in Fig. 8. Assuming that the ground state has a spin-parity of  $\frac{3}{2}^+$ , then

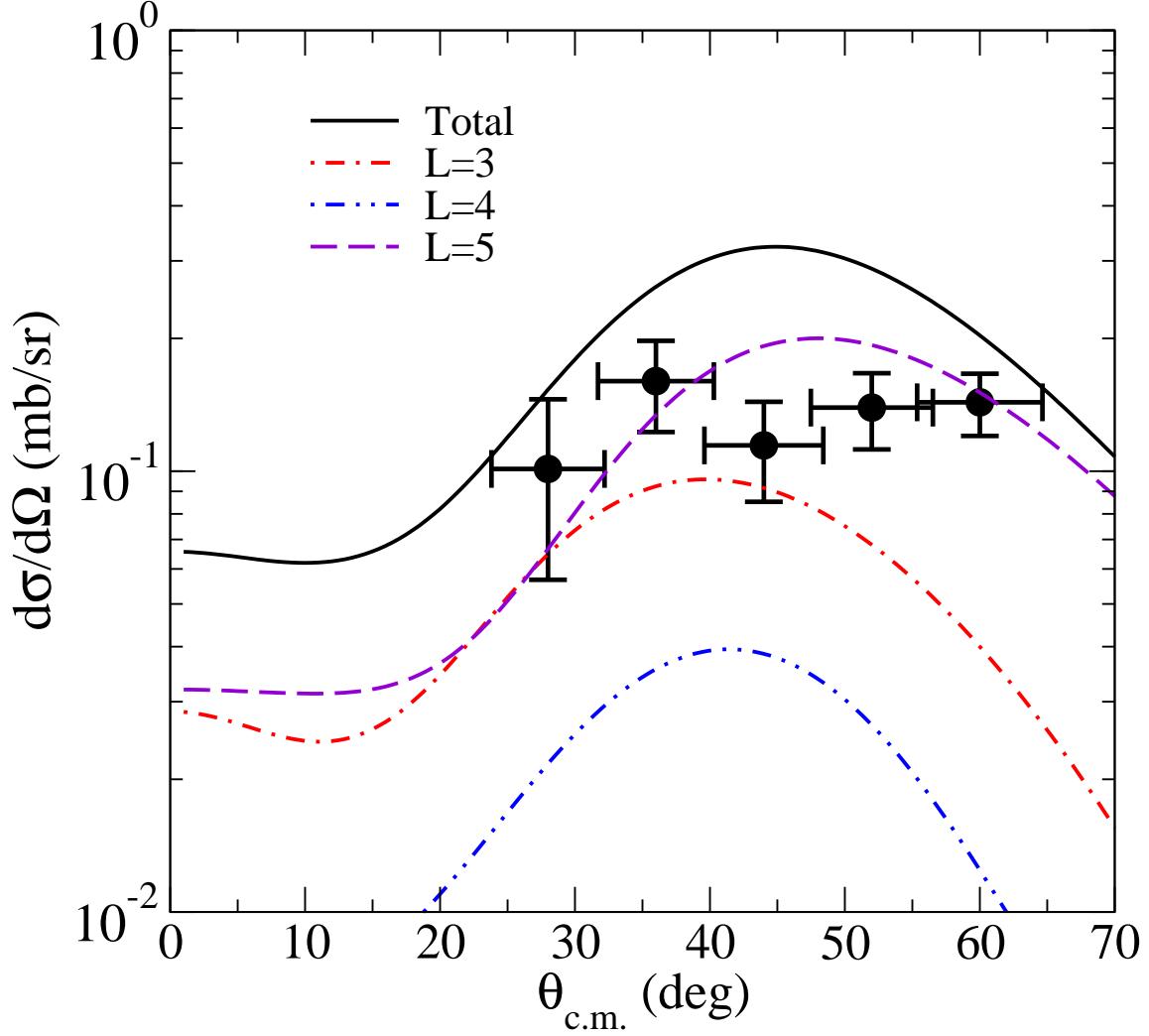


FIG. 8: (Color online.) The differential cross sections for the inelastic scattering of 70 MeV protons from  $^{17}\text{C}$  leading to the state at 3.05 MeV excitation. The legends identify which multipoles of the transition have been kept in the calculation. More details are given in the text.

transition multipoles ( $L$ ) of 3, 4, and 5 are possible. The angular-momentum allowed case of  $L = 6$  is not feasible given the single-particle basis used in the shell-model calculations. The total result is depicted by the solid curve in Fig. 8. The separate component cross sections are portrayed by the dot-dashed, the dot-dot-dashed, and the long-dashed curves for the  $L = 3, 4$ , and 5 contributions respectively. Clearly our prediction is slightly too large in comparison with the data, and it is the  $L = 5$  associated with recoupling of a  $d_{5/2}$  neutron orbit that is primarily responsible.

Satou *et al.* [3] also measured the cross section for the excitation of the 1.46 MeV state in  $^{19}\text{C}$  from the scattering of that ion from hydrogen. Those data are shown in Fig. 9. There are three evaluations with which these data are compared. Those depicted by the solid and long-dashed curves were made assuming that the ground state had a spin-parity of  $\frac{1}{2}^+$ . Both results are dominated by  $L = 2$  angular momentum transfer. The solid (dashed) curve is the result found using oscillator (Woods-Saxon) functions for the single-nucleon bound-state wave functions that reflect a neutron skin (halo-like) property to the density. The result



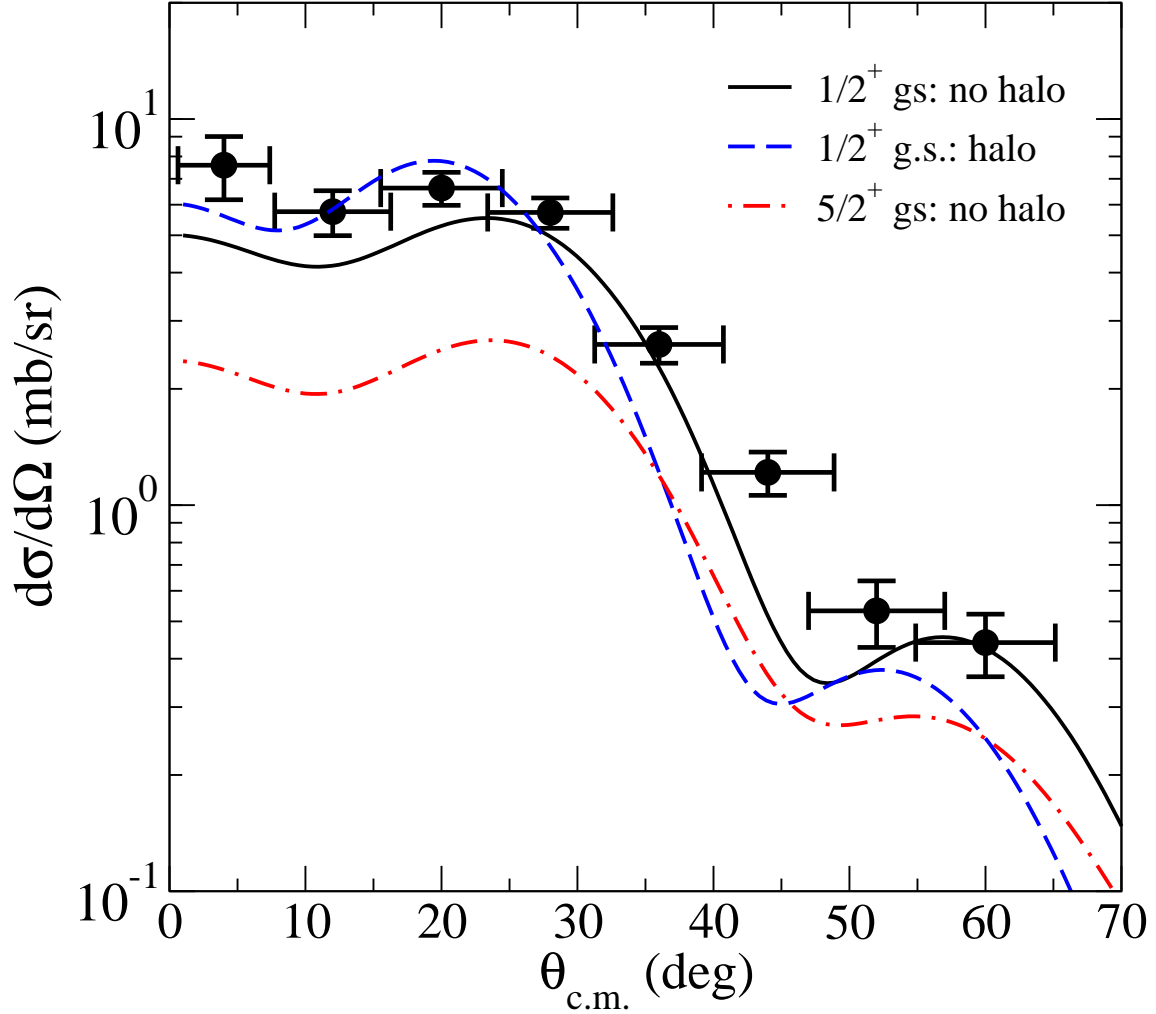


FIG. 9: (Color online.) The differential cross sections for the inelastic scattering of 70 MeV protons from  $^{19}\text{C}$  leading to the state at 1.46 MeV excitation. The legends indicate what has been assumed to be the spin-parity of the ground state and whether oscillator (no halo) or the Woods-Saxon (halo) functions were used. More details are given in the text.

depicted by the dot-dashed curve, was found using the oscillator wave functions but on assuming that the ground state had a spin-parity of  $\frac{5}{2}^+$ . These results indicate that the ground state of  $^{19}\text{C}$  has indeed the  $\frac{1}{2}^+$  assignment as has been suggested [3], but that it may have a neutron skin rather than a neutron halo. Again, measurement of the elastic scattering cross section may give a resolution between the alternatives for the extended distribution of neutrons in this ion.

## V. CONCLUSIONS

These studies of the spectra of  $^{17,19}\text{C}$ , made with quite complementary models (SM and MCAS) for their structure, reveal that they are very sensitive to details used in these models. This presents a very clear need for many more experimental studies of the systems to be made to enumerate many more states in their spectra, at low excitations especially, and to

determine the spin-parity assignments most appropriate for each state therein. Scattering data are also needed to provide the best possible test of the wave functions deemed most suited to describe the ions. In particular, cross sections from RIB elastic scattering from hydrogen targets, and eventually with electrons (as may be done using the self confining radioactive ion targets (SCRIT) system [31]), should be of most use given that the theories available to describe those reactions are formulated, currently, with least approximation problems.

## Acknowledgments

This research was supported by the Italian MIUR-PRIN Project “Fisica Teorica del Nucleo e dei Sistemi a Più Corpi”, by the Natural Sciences and Engineering Research Council (NSERC), Canada, by the National Research Foundation of South Africa, and by support from the International Exchange Program of the Australian Academy of Science.

- 
- [1] P. Hansen, A. S. Jensen, and B. Jonson, *Annu. Rev. Nucl. Part. Sci.* **45**, 2 (1995).
  - [2] T. Suzuki et al., in *Proceedings of the International Symposium on Frontiers of Collective Motions (CM2002)*, edited by H. Sagawa and H. Iwasaki (World Scientific, Singapore, 2003), p. 236.
  - [3] Y. Satou et al., *Phys. Lett.* **B660**, 320 (2008).
  - [4] T. Nakamura et al., *Phys. Rev. Lett.* **83**, 1112 (1999).
  - [5] T. Otsuka, R. Fujimoto, Y. Utsuno, B. A. Brown, M. Honma, and T. Mizusaki, *Phys. Rev. Lett.* **87**, 082502 (2001).
  - [6] P. Bannerjee and R. Shyam, *Phys. Rev. C* **61**, 047301 (2000).
  - [7] Z. Elekes et al., *Phys. Lett.* **B614**, 174 (2005).
  - [8] B. A. Brown, A. Etchegoyen, and W. D. M. Rae (1986), OXBASH-MSU (the Oxford Buenos-Aries Michigan State University shell model code) MSU-NSCL Report Number 524.
  - [9] E. K. Warburton and B. A. Brown, *Phys. Rev. C* **46**, 923 (1992).
  - [10] D. Ridikas, M. H. Smedberg, J. S. Vaagen, and M. V. Zhukov, *Europhys. Lett.* **37**, 97 (1997).
  - [11] D. Ridikas, M. H. Smedberg, J. S. Vaagen, and M. V. Zhukov, *Nucl. Phys.* **A628**, 363 (1998).
  - [12] L. Canton, G. Pisent, J. P. Svenne, D. van der Knijff, K. Amos, and S. Karataglidis, *Phys. Rev. Lett.* **94**, 122503 (2005).
  - [13] L. Canton, G. Pisent, K. Amos, S. Karataglidis, J. P. Svenne, and D. van der Knijff, *Phys. Rev. C* **74**, 064605 (2006).
  - [14] L. Canton, G. Pisent, J. P. Svenne, K. Amos, and S. Karataglidis, *Phys. Rev. Lett.* **96**, 072502 (2006).
  - [15] G. Pisent, J. P. Svenne, L. Canton, K. Amos, S. Karataglidis, and D. van der Knijff, *Phys. Rev. C* **72**, 014601 (2005).
  - [16] K. Amos, P. J. Dortmans, H. V. von Geramb, S. Karataglidis, and J. Raynal, *Adv. Nucl. Phys.* **25**, 275 (2000).
  - [17] A. Lagoyannis et al., *Phys. Lett.* **B518**, 27 (2001).
  - [18] S. V. Stepantsov et al., *Phys. Lett.* **B542**, 35 (2002).
  - [19] A. Ozawa et al., *Nucl. Phys.* **A691**, 599 (2001).

- [20] J. A. Tostevin and J. S. Al-Khalili, Phys. Rev. C **59**, R5 (1999).
- [21] P. J. Karol, Phys. Rev.C **11**, 1203 (1975).
- [22] E. Liatard et al., Europhys. Lett. **13**, 401 (1990).
- [23] M. Lassaut and R. J. Lombard, Z. Phys. A **341**, 125 (1992).
- [24] Z. Bazin et al., Phys. Rev. Lett. **74**, 3569 (1995).
- [25] K. Amos, W. A. Richter, S. Karataglidis, and B. A. Brown, Phys. Rev. Lett. **96**, 032503 (2006).
- [26] K. Amos, L. Canton, G. Pisent, J. P. Svenne, and D. van der Knijff, Nucl. Phys. **A728**, 65 (2003).
- [27] L. Canton, K. Amos, S. Karataglidis, G. Pisent, J. P. Svenne, and D. van der Knijff, Nucl. Phys. **A790**, 251c (2007).
- [28] D. R. Tilley, H. R. Weller, and C. M. Cheves, Nucl. Phys. **A564**, 1 (1995).
- [29] D. R. Tilley, H. R. Weller, C. M. Cheves, and R. M. Chasteler, Nucl. Phys. **A595**, 1 (1995).
- [30] K. Amos, S. Karataglidis, D. van der Knijff, L. Canton, G. Pisent, and J. P. Svenne, Phys. Rev. C **72**, 064604 (2005).
- [31] T. Suda and M. Wakasugi, Prog. Part. Nucl. Phys. **55**, 417 (2005).